

Geophysical Research Letters*



RESEARCH LETTER

10.1029/2025GL117660

Key Points:

- Applying a time-varying emergence constraint markedly reduces the projected sea ice concentration uncertainties in the Barents-Kara Sea
- For SSP5-8.5 and SSP3-7.0, the constrained ice-free ranges are delayed by about 18 years, with increased maximum ice-free probability
- For SSP2-4.5 and SSP1-2.6, the constrained ice-free range is shifted to the end of 21st century, with decreased maximum ice-free probability

Supporting Information:

Supporting Information may be found in the online version of this article.

Correspondence to:

A. Duan, amduan@xmu.edu.cn

Citation:

Peng, Y., Duan, A., Shen, Z., Wei, J., & Cao, S. (2025). Emergent constraint on CMIP6 model projections of winter ice-free periods in the Barents–Kara Sea. *Geophysical Research Letters*, 52, e2025GL117660. https://doi.org/10.1029/2025GL117660

Received 17 JUN 2025 Accepted 24 SEP 2025

Author Contributions:

Conceptualization: Yuzhuo Peng Funding acquisition: Anmin Duan Project administration: Anmin Duan Supervision: Anmin Duan Visualization: Yuzhuo Peng Writing – original draft: Yuzhuo Peng Writing – review & editing: Anmin Duan, Zili Shen, Jilin Wei, Shutao Cao

© 2025. The Author(s). This is an open access article under the terms of the Creative Commons Attribution License, which permits use, distribution and reproduction in any medium, provided the original work is properly cited.

Emergent Constraint on CMIP6 Model Projections of Winter Ice-Free Periods in the Barents–Kara Sea

Yuzhuo Peng¹, Anmin Duan¹, Zili Shen², Jilin Wei³, and Shutao Cao¹

¹Center for Marine Meteorology and Climate Change, State Key Laboratory of Marine Environmental Science, College of Ocean and Earth Sciences, Xiamen University, Xiamen, China, ²Institute of Atmospheric Sciences, Fudan University, Shanghai, China, ³State Key Laboratory of Earth System Numerical Modeling and Application, Institute of Atmospheric Physics, Chinese Academy of Sciences, Beijing, China

Abstract Severe winter ice loss in the Barents–Kara Sea (BKS) affects the local environment and climate in other regions. To reduce sea ice projection uncertainties and reliably identify future ice-free periods, we apply a time-varying emergent constraint method to model simulations from the Coupled Model Intercomparison Project Phase 6 (CMIP6). For SSP5-8.5, the constrained ice-free date is the multi-model ensemble mean (MMEM) estimate of 2071–2075 with a 90% confidence range (equivalent to IPCC's "very likely range") of [2047, 2100+], while it shifts to 2086–2090 with the very likely range of [2054, 2100+] for SSP3-7.0. For SSP2-4.5 and SSP1-2.6, the very likely range for the ice-free dates are [2080, 2100+] and [2095, 2100+], while ice remains in the optimal constrained MMEM sea ice concentration. Relative to the unconstrained results, the optimal constrained maximum probability of an ice-free BKS increases notably under SSP5-8.5 and SSP3-7.0, but decreases under SSP1-2.6 and SSP2-4.5.

Plain Language Summary The recent winter Barents–Kara Sea (BKS) sea ice concentration (SIC) decrease has considerably affected global weather and climate. Model projections from the Coupled Model Intercomparison Project Phase 6 (CMIP6) confirm a future decrease in BKS SIC, but the magnitude and characteristics of this decrease remain uncertain, complicating assessments of future ice-free conditions. Applying the time-varying emergent constraint method, future BKS SIC is constrained by the observation, thereby reducing projection uncertainty and offering a more reliable scientific basis for the timing of an ice-free period. After the constraint, the very likely ranges of the ice-free period under SSP1-2.6 and SSP2-4.5 become narrower and shift toward the end of the 21st century. Under SSP3-7.0 and SSP5-8.5, the constrained ranges show a delay of approximately 18 years in the onset of the ice-free condition compared to the original results. Additionally, the optimal constrained maximum ice-free probability increases to 67% and 63% for SSP5-8.5 and SSP3-7.0, respectively, up from 42% to 32% in the original projections. Conversely, the constrained probabilities under SSP1-2.6 and SSP2-4.5 are lower and suggest ice-free conditions are even unlikely. These results clearly underscore the crucial importance of greenhouse gas emission mitigation in slowing sea ice loss in the BKS.

1. Introduction

Although the Barents–Kara Sea (BKS) accounts for only 11% of the Arctic ocean (Meier & Stewart, 2023), it has contributed approximately 30%–40% of the total Arctic winter sea ice loss in recent years (Z. Liu et al., 2022; Onarheim et al., 2018). Recent studies have also reported that as the Arctic transitions to a seasonally ice-free state in the future, winter sea ice loss is expected to dominate, potentially rendering the region a tipping point in the climate system (McKay et al., 2022; Stroeve & Notz, 2018; Årthun et al., 2021). Consequently, recent severe winter sea ice loss in the BKS has attracted considerable attention from the scientific community (Dörr et al., 2024; Luo & Yao, 2018; Rieke et al., 2023; Tian et al., 2022; Yamagami et al., 2022).

Changes in winter BKS sea ice can substantially affect regional climate and ecological conditions. For instance, sea ice loss in this region can amplify surface air temperature warming (Dai et al., 2019; Dai & Jenkins, 2023; Jenkins & Dai, 2021), enhance primary productivity (Ardyna et al., 2014; Dalpadado et al., 2020; Ji et al., 2013), exacerbate ocean acidification (Årthun et al., 2025; Ericson et al., 2023; Qi et al., 2022), contribute to the northward migration of fish populations (Fall et al., 2018; Nascimento et al., 2023; Varpe et al., 2014), and produce a variety of other ecological and environmental impacts (Aune et al., 2021; Gerland et al., 2023; Strople et al., 2023; Toxværd et al., 2019). Moreover, the impact of winter BKS sea ice loss is not only local, but also

PENG ET AL.

influences weather and climate in distant regions (Delhaye et al., 2024; Ghosh et al., 2024; Jiang et al., 2021; Koenigk et al., 2016; Xinxin; Li et al., 2019; Mori et al., 2014, 2019; Petoukhov & Semenov, 2010; Vihma et al., 2014; Xu et al., 2021; Zhang, Wu, Simpson, et al., 2018; Zhang, Wu, & Smith, 2018). For example, Mori et al. (2014, 2019) demonstrated that winter BKS sea ice loss enhances the frequency of Eurasian blocking events, thereby facilitating the intrusion of cold air into Eurasia and contributing approximately 44% during 1995-2024 to the observed Eurasian cooling trend. Zhang, Wu, & Smith (2018) and Zhang, Wu, Simpson, et al. (2018) further revealed that early-winter BKS sea ice loss can induce cold advection over central Asia and lead to a colder Siberia, both primarily through stratosphere-troposphere coupling. Similarly, Sun et al. (2022) suggested that over the past two decades, the reduction in winter BKS sea ice increased the frequency of extreme heatwaves in the mid-high latitudes of Eurasia during spring by enhancing the troposphere-stratosphere interactions. Furthermore, Hou et al. (2022) showed that this ice loss triggers a wavenumber one atmospheric circulation, leading to cooling over Eurasia and warming over North America. More recently, Ghosh et al. (2024) further emphasized the role of winter BKS sea ice loss in the observed surface air temperature cooling trend over Eurasia in winter, noting a roughly 6-year cycle linked to the Warm-Arctic Cold-Eurasia pattern. Additionally, Cheng et al. (2025) depicted that the winter sea ice state in and around the Barents Sea acts is a significant precursor of the Indian Ocean Dipole development during the following autumn.

Additionally, recent studies have also explored the potential influence of BKS sea ice loss on climate change over the "Third Pole" — the Tibetan Plateau (TP). In particular, previous studies suggested that wintertime BKS sea ice reduction could enhance the transport of aerosols from South Asia to the TP (F. Li et al., 2020), intensifying winter warming (Duan et al., 2022) and snowmelt (Y. Chen et al., 2020) over the TP. Given that both Arctic sea ice and the TP are considered potential climate tipping elements, continued winter BKS sea ice loss could accelerate the progression of climate anomalies over the TP toward a critical threshold (T. Liu et al., 2023; McKay et al., 2022). These scientific results emphasize the impact of winter BKS sea ice loss on climate and ecological systems at the regional and global scales. Therefore, a comprehensive understanding of future winter sea ice evolution in the BKS—particularly the potential occurrence and timing ice-free conditions—is essential to support climate adaptation strategies and evidence-based policy decisions to prepare for sustainable development in the polar regions (Xin Li et al., 2025).

Given the importance of winter sea ice change in the BKS region and the timing of the transition to an ice-free state, several studies have sought to address this issue using the Coupled Model Intercomparison Project model datasets (Onarheim & Årthun, 2017; Pan et al., 2023; Peng et al., 2024). The previous study employed a 40-member ensemble of the Community Earth System Model and projected that, under Representative Concentration Pathway 8.5 (RCP8.5) scenario, the winter ice-free period in the Barents region would occur between 2061 and 2088 (Onarheim & Årthun, 2017). Subsequently, Pan et al. (2023) suggested that under Shared Socioeconomic Pathway 5–8.5 (SSP5-8.5) scenario, the winter ice-free condition of the Barents region may emerge between 2042 and 2089. A recent study reported that the winter BKS region would not experience an ice-free period under SSP1-2.6 scenario alone (Peng et al., 2024). While these studies provide valuable insights, it is important to recognize that the results could be influenced by model dependencies and associated uncertainties.

Recently, the emergent constraint method has been widely used to reduce projection uncertainty by leveraging a robust inter-model relationship between historical factor and future climate projection (Bracegirdle & Stephenson, 2013; Kwiatkowski et al., 2017; Yao et al., 2025; Zhu et al., 2024). However, in most studies employing the emergent constraint method, the selection of historical period used to constrain future projection was often arbitrary, depending primarily on the availability of observational data (Z. Chen et al., 2023; A. Liu et al., 2024; Shiogama et al., 2022; Terhaar et al., 2020), which could overlook the dynamic and evolving nature of the climate system over time. Shen et al. (2023) proposed a time-varying emergent constraint method, which can effectively address this issue by identifying the optimal historical constraint period corresponding to different future projection periods, thereby yielding more reasonable projection results. Therefore, to adopt a more objective constraint approach and consider the potential changes in the Arctic system, this study employs the time-varying emergent constraint method to estimate future winter BKS sea ice changes and access the emergence of ice-free conditions, with the goal of improving the robustness and credibility of climate projections.

PENG ET AL. 2 of 11

2. Data and Methods

2.1. Data

The observational sea ice concentration (SIC) with a $25 \text{ km} \times 25 \text{ km}$ grid during 1979-2024 is from Version 4 of the Climate Data Record of Passive Microwave SIC provided by the National Snow and Ice Data Center (NSIDC) (Meier et al., 2021). A regional mask for the BKS region, which serves as the focus area of this study, is also provided by NSIDC, as shown in Figure S1a in Supporting Information S1. Since satellite observation data of SIC commenced in 1979, our analysis focuses on the output after 1979, which is adopted in the previous studies (Liu et al., 2013; Onarheim & Årthun, 2017; Shen et al., 2021).

For model simulations, this study utilizes SIC data from 30 CMIP6 models (detailed, Table S1 in Supporting Information S1) under both historical simulations and future emission scenarios (Eyring et al., 2016; O'Neill et al., 2016). The future scenarios include SSP1-2.6, SSP2-4.5, SSP3-7.0, and SSP5-8.5, which represent different socioeconomic development and radiative forcing conditions. These scenarios are used to assess future changes of wintertime BKS SIC and to project the timing of potential ice-free condition. The first publicly available ensemble member is analyzed for each model (Table S1 in Supporting Information S1) and the winter BKS SIC time series is computed on the model's native grid. Here, a winter in the BKS is considered ice-free if the regional average SIC during that season falls below 15% for the first time, based on the value smoothed with a 5-year running mean (Årthun et al., 2021). The winter mean value is calculated as the seasonal mean value from the December, January, and February data.

2.2. Time-Varying Emergent Constraint Method

The traditional emergent constraint method consists of two main steps:

1. Identify a physically meaningful historical predictor (X) that exhibits a significant correlation with a future climate variable of interest (Y), and establish an inter-model linear regression relationship between them:

$$Y = \overline{Y} + b(X - \overline{X}) \tag{1}$$

Where b is the regression coefficient, \overline{Y} and \overline{X} is the multi-model mean of Y and X, respectively.

2. Apply this statistical relationship to constrain the future projection by substituting the observed value X_o into the regression equation to obtain the constrained Y_c , and subsequently calculate the associated prediction confidence interval:

$$Y_c = \overline{Y} + b(X_o - \overline{X}) \tag{2}$$

$$\sigma_{Y_c}^2 = \frac{\sum_{i=1}^n (Y_i - \overline{Y})^2}{n-2} (1 - r^2)$$
 (3)

Where r is the inter-model correlation coefficient between Y and X, n is the number of models, and $\sigma_{Y_c}^2$ is the constrained variance, respectively. According to the "very likely range" defined in the Intergovernmental Panel on Climate Change (IPCC) report (Masson-Delmotte et al., 2021), the 90% prediction confidence interval of Y_c is calculated here, that is $[Y_c - 1.65\sigma_{Y_c}, Y_c + 1.65\sigma_{Y_c}]$, assuming a normal distribution for the regression residuals.

More recently, the time-varying emergent constraint method has refined the traditional approach by evaluating inter-model correlations between the future predictand and the predictor over different historical periods. The period exhibiting the strongest correlation (i.e., the highest inter-model correlation coefficient) is identified as the optimal constraint window, within which the traditional emergent constraint method is subsequently applied for further analysis (Shen et al., 2023).

Additionally, the quantitative measure of the reduced uncertainty between the constrained and unconstrained results of winter BKS SIC is calculated as follows:

PENG ET AL. 3 of 11

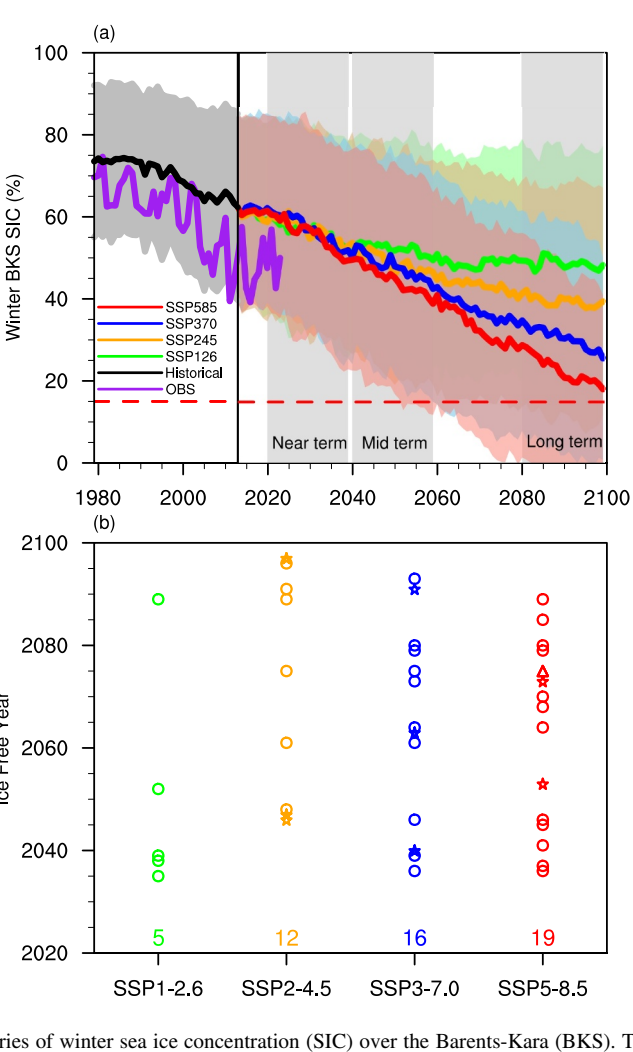


Figure 1. (a) The time series of winter sea ice concentration (SIC) over the Barents-Kara (BKS). The solid purple line represents the observed winter SIC from 1979 to 2023. The solid black, green, orange, blue, and red lines indicate the multimodel ensemble mean (MMEM) of 30 Coupled Model Intercomparison Project Phase 6 (CMIP6) models under the historical, SSP1-2.6, SSP2-4.5, SSP3-7.0 and SSP5-8.5 scenarios, respectively. The Shading shows the one standard deviation spread from the MMEM value. The horizontal dashed red line indicates the threshold for the ice-free condition. (b) The winter ice-free year over the BKS projected by 30 CMIP6 models under the four scenarios. The circle, pentagram, and triangle represent the year with one, two, and three models indicating ice-free condition, respectively. The green, orange, blue and red numbers denote the amount of 30 models projecting ice-free state under the four scenarios, respectively.

 $Reduced \ uncertainty = \frac{\text{uncontrained uncertainty range of SIC} - \text{contrained uncertainty range of SIC}}{\text{uncontrained uncertainty range of SIC}} \times 100\%$

(4)

19448007, 2025, 19, Downloaded from https://agupubs.onlinelibrary.wiley.com/doi/10.1029/2025GL117660 by Readcube (Labtiva Inc.), Wiley Online Library on [08/10/2025]. See the Terms

3. Results

3.1. Winter BKS SIC in Original CMIP6 Simulations

Figure 1a illustrates the time series of winter BKS SIC, where the purple line represents the observation and the black line corresponds to the multi-model ensemble mean (MMEM) derived from 30 CMIP6 models. During the historical simulation period (1979–2014), the MMEM exhibits a positive bias compared to the observation, with its climatological mean approximately 10% higher. In 2015–2023, the MMEM projections remain consistently higher than the observation under all emission scenarios, suggesting a possible delay in the occurrence of ice-free conditions in the BKS. Moreover, the MMEM SIC projections remain broadly consistent for all emission scenarios in the near-term period (2020–2039) but start diverging in the mid-term period (2040–2059). Toward the

PENG ET AL. 4 of 11

late 21st century (2080–2099), the winter BKS SIC stabilizes under SSP1-2.6 and SSP2-4.5 but decreases further under the SSP3-7.0 and SSP5-8.5 scenarios, in response to the continuously increasing greenhouse gas forcing. Nevertheless, the calculated SIC values remain above the 15% threshold, even under high-emission scenarios.

Shaded areas in Figure 1a indicates the range of uncertainty in winter BKS SIC projections derived from the CMIP6 models. There is a notable spread among the 30 models. The associated uncertainty increases substantially over time. This growing uncertainty directly contributes to the divergence in CMIP6 model projections regarding the timing of future winter ice-free conditions in the BKS region (Figure 1b). Specifically, only 5 models project an ice-free state in the BKS before 2100 under SSP1-2.6 scenario, with onset years from 2039 to 2089. Under SSP2-4.5, 12 models project ice-free conditions starting between 2046 and 2097, while 16 models simulate an ice-free state occurring between 2036 and 2093 under the SSP3-7.0 scenario. Finally, for the high-emission SSP5-8.5 scenario, 19 models indicate an onset of ice-free conditions in the BKS between 2036 and 2089. The substantial inter-model spread in the occurring timing of winter BKS ice-free conditions and the biases presented in the historical simulations of CMIP6 models demonstrate the limitations of unconstrained projection methods. To alleviate these, this study will employ a time-varying emergent constraint approach to calibrate model projections and optimize the reliability as much as possible.

3.2. Constrained Projections of Winter BKS SIC

Models with more historical sea ice typically exhibit weaker responses to greenhouse gas forcing and slower ice loss, retaining ice for longer periods. Therefore, following earlier studies (J. Liu et al., 2013; Shen et al., 2023), the historical winter BKS SIC climatology is applied as a constraint factor on future SIC projections in that area. Since the observational data is available until winter 2023, the calibration period for projections is defined as the winters from 2024 to 2099. Figure 2 illustrates the process of time-varying emergent constraint, employing the 5-year mean of winter BKS SIC during 2024–2028 under SSP3-7.0 scenario as an example. The first step involves identifying the optimal constraint window for this projection period. In Figure 2a, the *x*-axis represents the ending year of each historical running period, the *y*-axis denotes the length of the running window, and the color shading indicates the inter-model correlation coefficients between the historical running means over different time periods and the projected five-year average SIC for 2024–2028. For instance, the point at (2023, 45) in Figure 2a represents the inter-model correlation coefficient between the average SIC over 1979–2023 and that over 2024–2028. The highest correlation coefficient value (black dot in Figure 2a) marks the optimal constraint period for the selected projection window. In this example, we identify 2011–2023 as the optimal constraint period, with an inter-model correlation coefficient of 0.98.

In Figure 2b, the *x*-axis represents the average value of SIC during the optimal historical constraint period (2011–2023), while the *y*-axis denotes that for the projection period (2024–2028). Different symbols represent individual climate models. The red solid line indicates the regression relationship between the historical and projected SIC values across models, with the pink shaded area representing the 90% prediction confidence interval. The green vertical dashed line marks the observed mean SIC for 2011–2023, which serves as the constraint on the projected SIC for 2024–2028. Results show that the constrained MMEM SIC is approximately 45% (blue dashed line in Figure 2b), which is 15% lower than the original CMIP6 MMEM (60%, gray dashed line). The corresponding 90% confidence interval for the constrained result is (36%, 53%) (blue shading), representing a 78% uncertainty reduction relatively to the original CMIP6 confidence interval ((21%, 99%), gray shading). The probability density function in Figure 2c further illustrates that the inter-model uncertainty in the projected SIC for 2024–2028 is substantially reduced after applying the constraint. For other emission scenarios, applying the optimal emergent constraint for the same period similarly yields MMEM SIC values that are over 10% lower than the original CMIP6 MMEM, along with a reduction in projection uncertainty exceeding 70% (Figures S2–S4 in Supporting Information S1). These results clearly demonstrate the effectiveness of the time-varying emergent constraint method.

A similar analysis is conducted for the remaining projection 5-year moving periods, as shown in Figure S5 in Supporting Information S1, which demonstrates that the optimal constraint period evolves over time across the four emission scenarios. This temporal dependence justifies the necessity of dynamically identifying the optimal constraint window rather than arbitrarily adopting a fixed period as in previous studies (Z. Chen et al., 2023; A. Liu et al., 2024; Shiogama et al., 2022; Terhaar et al., 2020). Therefore, it is important to emphasize that a constraint period optimal for one target window may not be appropriate for another, particularly under different

PENG ET AL. 5 of 11

1944807, 2023, 19, Downloaded from https://aguputs.onlinelibrary.viley.com/doi/10.1029/2025GL117660 by Readcube (Labtiva Inc.), Wiley Online Library on [08/10/2025], See the Terms and Conditions (thtps://onlinelibrary.wiley.com/terms-and-conditions) on Wiley Online Library on [08/10/2025], See the Terms and Conditions (thtps://onlinelibrary.wiley.com/terms-and-conditions) on Wiley Online Library on [08/10/2025], See the Terms and Conditions (thtps://onlinelibrary.wiley.com/terms-and-conditions) on Wiley Online Library on [08/10/2025], See the Terms and Conditions (thtps://onlinelibrary.wiley.com/terms-and-conditions) on Wiley Online Library on [08/10/2025], See the Terms and Conditions (thtps://onlinelibrary.wiley.com/terms-and-conditions) on Wiley Online Library on [08/10/2025], See the Terms and Conditions (thtps://onlinelibrary.wiley.com/terms-and-conditions) on Wiley Online Library on [08/10/2025], See the Terms and Conditions (thttps://onlinelibrary.wiley.com/terms-and-conditions) on Wiley Online Library on [08/10/2025], See the Terms and Conditions (thttps://onlinelibrary.wiley.com/terms-and-conditions) on Wiley Online Library on [08/10/2025], See the Terms and Conditions (thttps://onlinelibrary.wiley.com/terms-and-conditions) on Wiley Online Library on [08/10/2025], See the Terms and Conditions (thttps://onlinelibrary.wiley.com/terms-and-conditions) on Wiley Online Library on [08/10/2025], See the Terms and Conditions (thttps://onlinelibrary.wiley.com/terms-and-conditions) on Wiley Online Library on [08/10/2025], See the Terms and Conditions (thttps://onlinelibrary.wiley.com/terms-and-conditions) on Wiley Online Library on [08/10/2025], See the Terms and Conditions (thttps://onlinelibrary.wiley.com/terms-and-conditions) on Wiley Online Library on [08/10/2025], See the Terms and Conditions (thttps://onlinelibrary.wiley.com/terms-and-conditions) on Wiley Online Library on [08/10/2025], See the Terms and Conditions (thttps://onlinelibrary.wiley.com/terms-and-conditions) on Wiley Online Library on [08/10/202

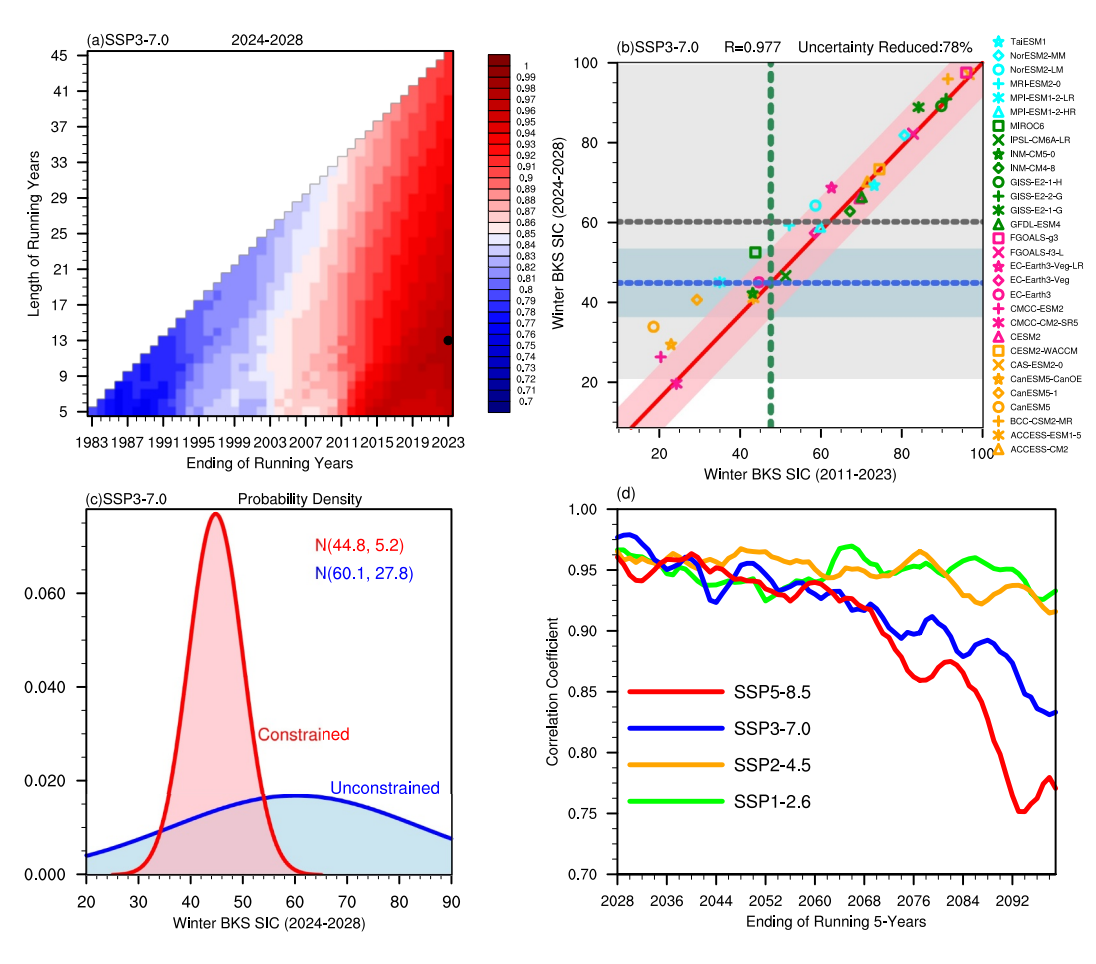


Figure 2. (a) The inter-model correlation coefficients between the running sea ice concentration (SIC) values over different periods during 1979–2023 and the projected SIC during 2024–2028 under SSP3-7.0 scenario. The black dot denotes the position of the maximum correlation coefficient, which is 0.977. (b) The result of constraining the projected SIC (2024–2028) using the observed SIC from the optimal constraint period (2011–2023) under SSP3-7.0 scenario. The solid pink line illustrates the regression line between the two, and the pink shading indicates the 90% prediction confidence interval. The green vertical dashed line marks the observation value. The blue dashed line depicts the constrained SIC, while the gray dashed line shows the original CMIP6 multi-model ensemble mean value. The 90% confidence interval of the constrained SIC is represented by the blue shading, and the original range is depicted by the gray shading. (c) The constrained (red) and original (blue) Probability density functions for winter SIC during 2024–2028. (d) Evolutions of the inter-model correlation coefficients between the optimal constraint period and the corresponding projected SIC during 2028–2099 under the four scenarios.

forcing scenarios. Reliance on a static constraint period could yield less reliable or even misleading projections. Moreover, Figure 2d illustrates the temporal evolution of inter-model correlation coefficients between the optimal constraint period and the corresponding projected values. Under SSP1-2.6 and SSP2-4.5 scenarios, correlation coefficients remain consistently above 0.9, indicating strong inter-model consistency. Conversely, under high-emission scenarios such as SSP3-7.0 and SSP5-8.5, the correlation coefficients exhibit a slight decline in the later period. Nevertheless, the correlation coefficients remain still above 0.75 and are statistically significant at the 99% confidence level, suggesting that the selected optimal constraint period maintains strong constraining ability across all scenarios.

Figure 3 compares times series of the projected winter BKS SIC with and without the emergent constraint. The gray shading and black line represent the original model ensemble results, whereas the colored shading and lines indicate the constrained projections. Applying the constraint leads to a substantial reduction in projection uncertainty and a systematic narrowing and temporal shift of the very likely range for the projected ice-free period. Specifically, under the SSP1-2.6 and SSP2-4.5 scenarios, the projected range of ice-free conditions changes from [2036, 2100+] to [2095, 2100+] and from [2034, 2100+] to [2080, 2100+], respectively. In contrast, the range

PENG ET AL. 6 of 11

19448007, 2025, 19, Downloaded from https://agupubs.onlinelibrary.wiley.com/doi/10.1029/2025GL117660 by Readcube (Labtiva Inc.), Wiley Online Library on [08/10/2025]. See the Terms

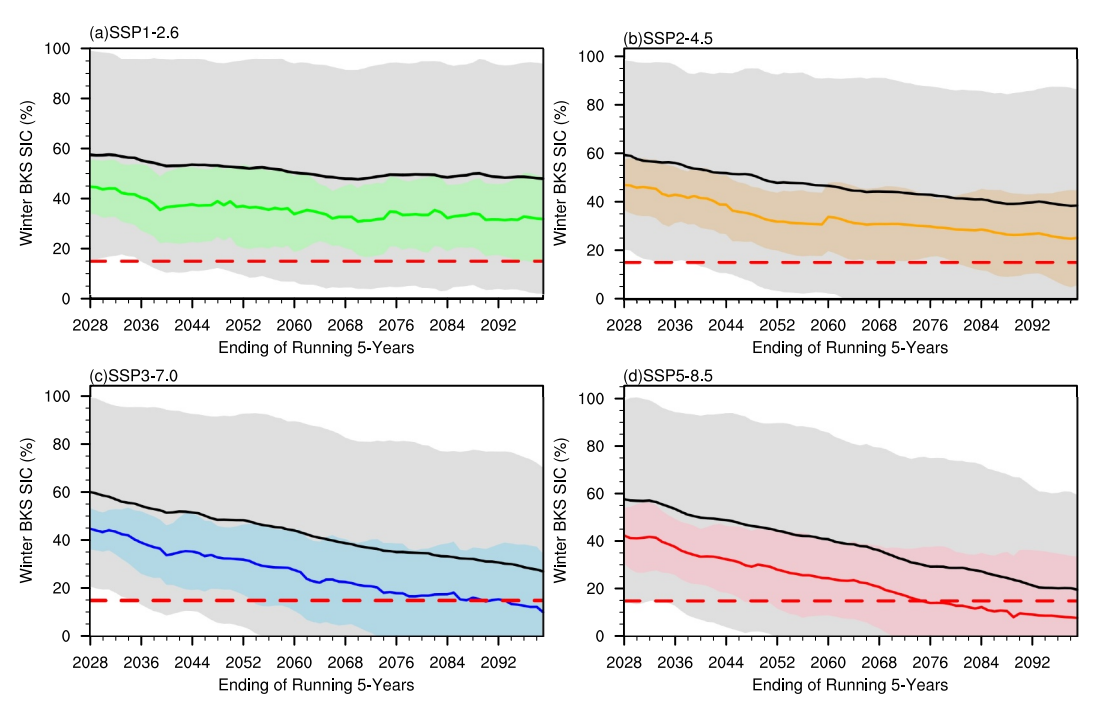


Figure 3. (a) The times series of the 5-year running winter Barents–Kara Sea sea ice concentration (SIC) during 2028–2099 under SSP1-2.6 scenario. The solid green line shows the optimal constrained SIC, while the gray dashed line shows the original CMIP6 multi-model ensemble mean value. The 90% confidence interval of the constrained SIC is represented by the green shading, and the original range is depicted by the gray shading. The horizontal dashed red line indicates the threshold for the ice-free condition. (b), (c), and (d) are same as (a) but for the results for SSP2-4.5, SSP3-7.0 and SSP5-8.5, respectively.

shifts from [2036, 2100+] to [2054, 2100+] under SSP3-7.0, and from [2029, 2100+] to [2047, 2100+] under SSP5-8.5. Furthermore, although the original MMEM projections indicate that an ice-free state does not occur under any scenario, the constrained MMEM projections show a further decrease in winter BKS SIC, with ensemble mean values reduced by 11%-19% depending on the scenario. This resulted notably in the emergence of ice-free conditions under SSP3-7.0 and SSP5-8.5, with ice-free periods occurring in [2086, 2090] and [2071, 2075], respectively. Additionally, Figure 4 further compares the optimal constrained and original results for the occurrence probability of the winter BKS ice-free conditions across all emission scenarios. According to the IPCC report, event likelihoods are categorized based on probability ranges as follows: 0%-10% (very unlikely), 10%-33% (unlikely), 33%-66% (likely as not), and 66%-100% (likely). Under the SSP5-8.5 scenario, the constrained results indicate that the probability of an ice-free winter in the BKS reaches the as likely as not level by 2069, occurring 17 years earlier than in the original results. By the end of the century, this probability further increases to the likely level, with a maximum probability of 68% compared to only 42% in the original projections. Under the SSP3-7.0 scenario, the constrained probability surpasses the as likely as not threshold in 2074, peaking at 63%, whereas the original projections remain within the unlikely range throughout the 21st century. In contrast, under SSP1-2.6 and SSP2-4.5 scenarios, the constrained probabilities remain consistently lower than their original counterparts, indicating that ice-free winters in the BKS are unlikely to occur during the 21st century.

4. Discussion and Conclusions

The rapid decline in winter BKS SIC has raised increasing scientific and societal concern because of its farreaching implications for the local climate and ecosystems, as well as for weather and climate patterns in remote regions. Nevertheless, future projections of winter BKS SIC remain highly uncertain across climate models, thereby constraining the robustness of climate impact assessments and adaptation planning. To address this issue, the present study employs the time-varying emergent constraint approach to CMIP6 model outputs, effectively reducing projection uncertainties and yielding more reliable results of future sea ice conditions.

PENG ET AL. 7 of 11

19448007, 2025, 19, Downloaded from https://agupubs.onlinelibrary.wiley.com/doi/10.1029/2025GL117660 by Readcube (Labtiva Inc.), Wiley Online Library on [08/10/2025]. See the Terms

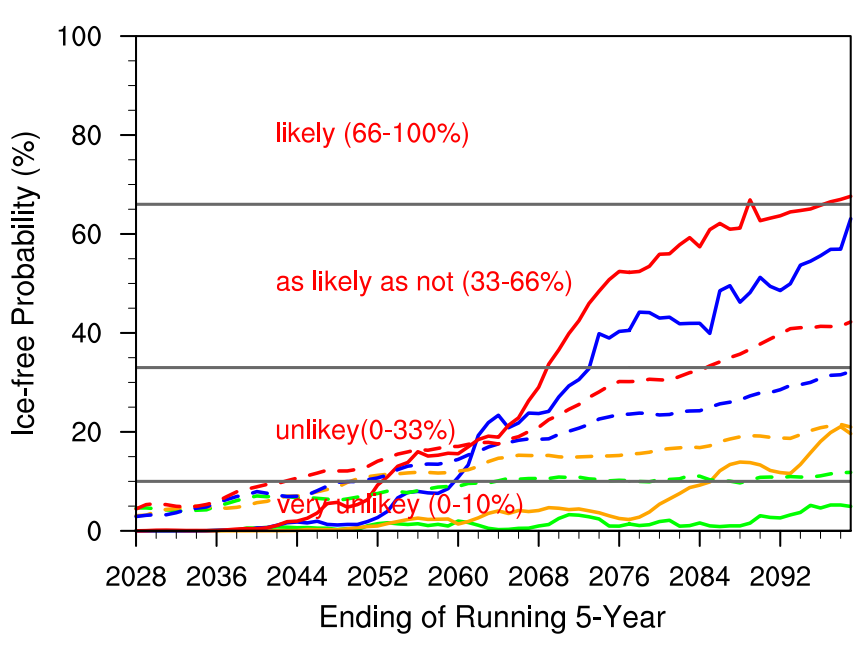


Figure 4. The winter ice-free probability for each year during 2028–2099 under the SSP1-2.6 (green), SSP2-4.5(orange), SSP3-7.0 (blue) and SSP5-8.5 (red), respectively. The solid lines indicate the results after constraint, and the dashed lines represent the original results. The Intergovernmental Panel on Climate Change report defines different terms according to the range of probability values, namely very unlikely (0%–10%), unlikely (0%–33%), as likely as not (33%–66%), likely (66%–100%).

Winter MMEM BKS SIC from the unconstrained CMIP6 output indicates no possibility of an ice-free period in that region, regardless of the future emission scenario. However, the optimally constrained results suggest that an ice-free period is projected to occur in 2086–2090 under SSP3-7.0 and in 2071–2075 under SSP5-8.5. For the low or moderate emission scenarios, applying the emergent constraint does not generate winter ice-free conditions in the BKS but the constrained MMEM SIC also decreases relatively to the original CMIP6 projections, by 10%–17%. Additionally, applying the constraint results in a pronounced narrowing and temporal shift of the very likely ranges for ice-free conditions. Specifically, the ranges shift from [2036, 2100+] to [2095, 2100+] under SSP1-2.6, from [2034, 2100+] to [2080, 2100+] under SSP2-4.5, from [2036, 2100+] to [2054, 2100+] under SSP3-7.0, and from [2029, 2100+] to [2047, 2100+] under SSP5-8.5. Furthermore, under SSP5-8.5 and SSP3-7.0, the optimally constrained maximum probability of an ice-free BKS rises markedly to 67% and 63%, respectively, compared with 42% and 32% in the original projections. In contrast, under SSP1-2.6 and SSP2-4.5, the constrained probabilities are reduced, suggesting that the occurrence of ice-free conditions becomes even less likely after applying the constraint.

To further evaluate the influence of constraint periods, a constraint using the 5-year mean of SIC from the most recent period (2019–2023) is employed as a fixed observational factor, to compare with the results based on the optimal constraint period. Firstly, Figure S6 in Supporting Information S1 analyzes the winter BKS SIC for 2024–2028 under different scenarios, constrained by the period 2019–2023. The uncertainty results decrease to 68.6%, 68.2%, 74.8%, and 62.7% under the SSP1-2.6, SSP2-4.5, SSP3-7.0 and SSP5-8.5 scenarios, respectively. In contrast, the corresponding reduced uncertainties after applying the optimal constraint period are 74%, 73%, 78%, and 72%, respectively. Moreover, Figure S7 in Supporting Information S1 shows that the inter-model correlation coefficients between the optimal constraint period and the corresponding projected SIC for 2028–2099 are higher than those obtained when using 2019–2023 as the constrained period. With the fixed constraint period, the constrained MMEM SIC also decreases for all scenarios (Figure S8 in Supporting Information S1), but generally less than that with the optimal constraint period. Consequently, an ice-free period emerges only under SSP5-8.5, occurring between 2085 and 2089, with the very likely ranges of ice-free conditions under all scenarios being delayed. Finally, Figure S9 in Supporting Information S1 confirms that the ice-free probabilities under all four scenarios are consistently lower when using the fixed constraint period than when applying the optimal constraint period. These findings highlight both the value of time-varying emergent constraint methods in improving sea ice

PENG ET AL. 8 of 11

19448007, 2025, 19, Downlo

doi/10.1029/2025GL117660 by Readcube (Labtiva Inc.)

Acknowledgments

This work was supported by the National

Science Foundation (2023M742910), the

Outstanding Postdoctoral Scholarship of

University, and the Open Project of the

Department of Atmospheric and Oceanic

OP202405). We thank Eric Dupuy, Ph.D., from Liwen Bianji (Edanz) (www.

liwenbianii.cn), for editing the English text

of a draft of this manuscript.

Sciences at Fudan University (FDAOS-

Natural Science Foundation of China

(42030602), the China Postdoctoral

the State Key Laboratory of Marine

Environmental Science at Xiamen

projections and the critical importance of greenhouse gas mitigation in delaying, or even preventing, an ice-free winter in the BKS.

However, the slight decline in inter-model correlations under the high-emission scenarios in the later years (Figure 2d) warrants further consideration. Although the correlation remains statistically significant and consistently above 0.75, which supports the continued reliability of the optimal constraint period, the reduced strength may reflect emerging differences in the dominant drivers of winter BKS SIC, such as atmospheric circulation (Z. Liu et al., 2022; Luo et al., 2023; Zhang et al., 2023) and oceanic heat transport (Årthun et al., 2019; D. Li et al., 2017; Yamagami et al., 2022), relative to the historical period. Further research is needed to investigate how such evolving mechanisms may influence the winter BKS SIC under the high-emission scenarios, with the aim of enhancing the reliability of future sea ice projection as much as possible and advancing our understanding for winter sea ice loss in the BKS region.

Conflict of Interest

The authors declare no conflicts of interest relevant to this study.

Data Availability Statement

The Arctic SIC are available from Meier et al. (2021) and the Arctic mask data can be obtained from https://daacdata.apps.nsidc.org/pub/DATASETS/nsidc0780_seaice_masks_v1/netcdf/. The CMIP6 mode outputs can be accessed through https://pcmdi.llnl.gov/CMIP6/.

References

Ardyna, M., Babin, M., Gosselin, M., Devred, E., Rainville, L., & Tremblay, J. É. (2014). Recent Arctic Ocean sea ice loss triggers novel fall phytoplankton blooms. *Geophysical Research Letters*, 41(17), 6207–6212. https://doi.org/10.1002/2014GL061047

Årthun, M., Dinh, K. V., Dörr, J., Dupont, N., Fransner, F., Nilsen, I., et al. (2025). The future Barents Sea- A synthesis of physical, biogeochemical, and ecological changes toward 2050 and 2100. Elementa, 13(1), 1–17. https://doi.org/10.1525/elementa.2024.00046

Årthun, M., Eldevik, T., & Smedsrud, L. H. (2019). The role of Atlantic heat transport in future arctic winter sea ice loss. *Journal of Climate*, 32(11), 3327–3341. https://doi.org/10.1175/JCLI-D-18-0750.1

Årthun, M., Onarheim, I. H., Dörr, J., & Eldevik, T. (2021). The seasonal and regional transition to an ice-free arctic. *Geophysical Research Letters*, 48(1), e2020GL090825. https://doi.org/10.1029/2020GL090825

Aune, M., Raskhozheva, E., Andrade, H., Augustine, S., Bambulyak, A., Camus, L., et al. (2021). Distribution and ecology of polar cod (boreogadus saida) in the eastern Barents Sea: A review of historical literature. *Marine Environmental Research*, 166, 105262. https://doi.org/10.1016/j.marenyres.2021.105262

Bracegirdle, T. J., & Stephenson, D. B. (2013). On the robustness of emergent constraints used in multimodel climate change projections of arctic warming. *Journal of Climate*, 26(2), 669–678. https://doi.org/10.1175/JCLI-D-12-00537.1

Chen, Y., Duan, A., & Li, D. (2020). Atmospheric bridge connecting the Barents Sea ice and snow depth in the mid-west Tibetan Plateau. Frontiers in Earth Science, 8, 265. https://doi.org/10.3389/feart.2020.00265

Chen, Z., Zhou, T., Chen, X., Zhang, W., Zuo, M., Man, W., & Qian, Y. (2023). Emergent constrained projections of mean and extreme warming in China. Geophysical Research Letters. 50(20), e2022GL102124. https://doi.org/10.1029/2022GL102124

Cheng, X., Chen, S., Chen, W., Wu, R., Ding, S., Zhou, W., et al. (2025). Influence of winter Arctic Sea ice anomalies on the following autumn Indian Ocean dipole development. *Journal of Climate*, 38(13), 3109–3129. https://doi.org/10.1175/jcli-d-24-0419.1

Dai, A., & Jenkins, M. T. (2023). Relationships among Arctic warming, sea-ice loss, stability, lapse rate feedback, and Arctic amplification. Climate Dynamics, 61(11–12), 5217–5232. https://doi.org/10.1007/s00382-023-06848-x

Dai, A., Luo, D., Song, M., & Liu, J. (2019). Arctic amplification is caused by sea-ice loss under increasing CO₂. *Nature Communications*, 10(1), 121. https://doi.org/10.1038/s41467-018-07954-9

Dalpadado, P., Arrigo, K. R., van Dijken, G. L., Skjoldal, H. R., Bagøien, E., Dolgov, A. V., et al. (2020). Climate effects on temporal and spatial dynamics of phytoplankton and zooplankton in the Barents Sea. *Progress in Oceanography*, 185, 102320. https://doi.org/10.1016/j.pocean. 2020.102320

Delhaye, S., Massonnet, F., Fichefet, T., Msadek, R., Terray, L., & Screen, J. (2024). Dominant role of early winter Barents-Kara sea ice extent anomalies in subsequent atmospheric circulation changes in CMIP6 models. *Climate Dynamics*, 62(4), 2755–2778. https://doi.org/10.1007/s00382-023-06904-6

Dörr, J., Årthun, M., Docquier, D., Li, C., & Eldevik, T. (2024). Causal links between sea-ice variability in the Barents-Kara Seas and Oceanic and atmospheric drivers. *Geophysical Research Letters*, 51(7), 1–12. https://doi.org/10.1029/2024GL108195

Duan, A., Peng, Y., Liu, J., Chen, Y., Wu, G., Holland, D. M., et al. (2022). Sea ice loss of the Barents-Kara Sea enhances the winter warming over the Tibetan Plateau. *Npj Climate and Atmospheric Science*, 5(1), 26. https://doi.org/10.1038/s41612-022-00245-7

Ericson, Y., Fransson, A., Chierici, M., Jones, E. M., Skjelvan, I., Omar, A., et al. (2023). Rapid fCO₂ rise in the northern Barents Sea and Nansen Basin. *Progress in Oceanography*, 217, 103079. https://doi.org/10.1016/j.pocean.2023.103079

Eyring, V., Bony, S., Meehl, G. A., Senior, C. A., Stevens, B., Stouffer, R. J., & Taylor, K. E. (2016). Overview of the Coupled Model Intercomparison Project Phase 6 (CMIP6) experimental design and organization. *Geoscientific Model Development*, 9(5), 1937–1958. https://doi.org/10.5194/gmd-9-1937-2016

Fall, J., Ciannelli, L., Skaret, G., & Johannesen, E. (2018). Seasonal dynamics of spatial distributions and overlap between northeast arctic cod (Gadus morhua) and capelin (Mallotus villosus) in the Barents Sea. *PLoS One*, 13(10), e0205921. https://doi.org/10.1371/journal.pone. 0205921

PENG ET AL. 9 of 11

19448007, 2025,



Geophysical Research Letters

- 10.1029/2025GL117660
- Gerland, S., Ingvaldsen, R. B., Reigstad, M., Sundfjord, A., Bogstad, B., Chierici, M., et al. (2023). Still Arctic? the changing Barents Sea. *Elementa*, 11(1), 00088, https://doi.org/10.1525/elementa.2022.00088
- Ghosh, R., Manzini, E., Gao, Y., Gastineau, G., Cherchi, A., Frankignoul, C., et al. (2024). Observed winter barents Kara sea ice variations induce prominent sub-decadal variability and a multi-decadal trend in the Warm arctic cold Eurasia pattern. *Environmental Research Letters*, 19(2), 024018. https://doi.org/10.1088/1748-9326/ad1c1a
- Hou, Y., Cai, W., Holland, D. M., Cheng, X., Zhang, J., Wang, L., et al. (2022). A surface temperature dipole pattern between Eurasia and North America triggered by the barents-kara sea-ice retreat in boreal winter. *Environmental Research Letters*, 17(11), 114047. https://doi.org/10.1088/1748-9326/ac9ecd
- Jenkins, M., & Dai, A. (2021). The impact of sea-ice loss on arctic climate feedbacks and their role for arctic amplification. *Geophysical Research Letters*, 48(15), e2021GL094599. https://doi.org/10.1029/2021GL094599
- Ji, R., Jin, M., & Varpe, Ø. (2013). Sea ice phenology and timing of primary production pulses in the Arctic Ocean. *Global Change Biology*, 19(3), 734–741. https://doi.org/10.1111/gcb.12074
- Jiang, Z., Feldstein, S. B., & Lee, S. (2021). Two atmospheric responses to winter sea ice decline over the barents-kara seas. Geophysical Research Letters, 48(7), e2020GL090288. https://doi.org/10.1029/2020GL090288
- Koenigk, T., Caian, M., Nikulin, G., & Schimanke, S. (2016). Regional arctic sea ice variations as predictor for winter climate conditions. *Climate Dynamics*, 46(1–2), 317–337. https://doi.org/10.1007/s00382-015-2586-1
- Kwiatkowski, L., Bopp, L., Aumont, O., Ciais, P., Cox, P. M., Laufkötter, C., et al. (2017). Emergent constraints on projections of declining primary production in the tropical oceans. *Nature Climate Change*, 7(5), 355–358. https://doi.org/10.1038/nclimate3265
- Li, D., Zhang, R., & Knutson, T. R. (2017). On the discrepancy between observed and CMIP5 multi-model simulated Barents Sea winter sea ice decline. Nature Communications, 8(1), 14991. https://doi.org/10.1038/ncomms14991
- Li, F., Wan, X., Wang, H., Orsolini, Y. J., Cong, Z., Gao, Y., & Kang, S. (2020). Arctic sea-ice loss intensifies aerosol transport to the Tibetan Plateau. *Nature Climate Change*, 10(11), 1037–1044. https://doi.org/10.1038/s41558-020-0881-2
- Li, X., Guo, H., Cheng, G., Song, X., Ran, Y., Feng, M., et al. (2025). Polar regions are critical in achieving global sustainable development goals. Nature Communications, 16(1), 1–12. https://doi.org/10.1038/s41467-025-59178-3
- Li, X., Wu, Z., & Li, Y. (2019). A link of China warming hiatus with the winter sea ice loss in barents–kara seas. Climate Dynamics, 53(5–6), 2625–2642. https://doi.org/10.1007/s00382-019-04645-z
- Liu, A., Xue, D., Chen, X., & Huang, D. (2024). Emergent constraints on the future East Asian winter surface air temperature changes. Environmental Research Letters, 19(6), 064050. https://doi.org/10.1088/1748-9326/ad4a91
- Liu, J., Song, M., Horton, R. M., & Hu, Y. (2013). Reducing spread in climate model projections of a September ice-free arctic. Proceedings of the National Academy of Sciences of the United States of America, 110(31), 12571–12576. https://doi.org/10.1073/pnas.1219716110
- Liu, T., Chen, D., Yang, L., Meng, J., Wang, Z., Ludescher, J., et al. (2023). Teleconnections among tipping elements in the Earth system. *Nature*
- Climate Change, 13(1), 67–74. https://doi.org/10.1038/s41558-022-01558-4

 Liu, Z., Risi, C., Codron, F., Jian, Z., Wei, Z., He, X., et al. (2022). Atmospheric forcing dominates winter barents-kara sea ice variability on intercompute to decoded time codes. Proposition of the National Academy of Sciences of the United States of America, 14(26), e2120770110.
- interannual to decadal time scales. *Proceedings of the National Academy of Sciences of the United States of America*, 119(36), e2120770119. https://doi.org/10.1073/pnas.2120770119
- Luo, B., Luo, D., Ge, Y., Dai, A., Wang, L., Simmonds, I., et al. (2023). Origins of barents-kara sea-ice interannual variability modulated by the Atlantic pathway of El Niño-southern Oscillation. *Nature Communications*, 14(1), 585. https://doi.org/10.1038/s41467-023-36136-5
- Luo, B., & Yao, Y. (2018). Recent rapid decline of the arctic winter Sea ice in the Barents-Kara seas owing to combined effects of the ural blocking and SST. *Journal of Meteorological Research*, 32(2), 191–202. https://doi.org/10.1007/s13351-018-7104-z
- Masson-Delmotte, V., Zhai, P., Pirani, A., Connors, S. L., Péan, C., Berger, S., et al. (2021). Climate change 2021: The physical science basis. Contribution of working group I to the sixth assessment report of the intergovernmental panel on climate change. Cambridge Univ. Press. 2391
- McKay, D. I. A., Staal, A., Abrams, J. F., Winkelmann, R., Sakschewski, B., Loriani, S., et al. (2022). Exceeding 1.5°C global warming could trigger multiple climate tipping points. *Science*, 377(6611), eabn7950. https://doi.org/10.1126/science.abn7950
- Meier, W. N., Fetterer, F., Windnagel, A. K., & Stewart, J. S. (2021). NOAA/NSIDC climate data record of passive microwave sea ice concentration. (G02202, version 4) [DataSet]. *National Snow and Ice Data Center*. https://doi.org/10.7265/efmz-2t65
- Meier, W. N., & Stewart, J. S. (2023). Arctic and antarctic regional masks for sea ice and related data products, version 1. National Snow and Ice Data Center. https://doi.org/10.5067/CYW3O8ZUNIWC
- Mori, M., Kosaka, Y., Watanabe, M., Nakamura, H., & Kimoto, M. (2019). A reconciled estimate of the influence of arctic sea-ice loss on recent Eurasian cooling. *Nature Climate Change*, 9(2), 123–129. https://doi.org/10.1038/s41558-018-0379-3
- Mori, M., Watanabe, M., Shiogama, H., Inoue, J., & Kimoto, M. (2014). Robust arctic sea-ice influence on the frequent Eurasian cold winters in past decades. *Nature Geoscience*, 7(12), 869–873. https://doi.org/10.1038/ngeo2277
- Nascimento, M. C., Husson, B., Guillet, L., & Pedersen, T. (2023). Modelling the spatial shifts of functional groups in the Barents Sea using a climate-driven spatial food web model. *Ecological Modelling*, 481, 110358. https://doi.org/10.1016/j.ecolmodel.2023.110358
- Onarheim, I. H., & Årthun, M. (2017). Toward an ice-free Barents Sea. Geophysical Research Letters, 44(16), 8387–8395. https://doi.org/10.1002/2017GL074304
- Onarheim, I. H., Eldevik, T., Smedsrud, L. H., & Stroeve, J. C. (2018). Seasonal and regional manifestation of arctic sea ice loss. *Journal of Climate*, 31(12), 4917–4932. https://doi.org/10.1175/JCLI-D-17-0427.1
- O'Neill, B. C., Tebaldi, C., Van Vuuren, D. P., Eyring, V., Friedlingstein, P., Hurtt, G., et al. (2016). The scenario model intercomparison project (ScenarioMIP) for CMIP6. Geoscientific Model Development, 9(9), 3461–3482. https://doi.org/10.5194/gmd-9-3461-2016
- Pan, R., Shu, Q., Song, Z., Wang, S., He, Y., & Qiao, F. (2023). Simulations and projections of winter sea ice in the Barents Sea by CMIP6 climate models. *Advances in Atmospheric Sciences*, 40(12), 2318–2330. https://doi.org/10.1007/s00376-023-2235-2
- Peng, Y., Duan, A., Shen, Z., Yao, Y., Yang, X., Hu, Z., & Yu, W. (2024). Projection of a winter ice-free barents-kara sea by CMIP6 models with the CCHZ-DISO method. *Atmospheric Research*, 310, 107631. https://doi.org/10.1016/j.atmosres.2024.107631
- Petoukhov, V., & Semenov, V. A. (2010). A link between reduced barents-kara sea ice and cold winter extremes over northern continents. *Journal of Geophysical Research*, 115(21), 1–11. https://doi.org/10.1029/2009JD013568
- Qi, D., Wu, Y., Chen, L., Cai, W. J., Ouyang, Z., Zhang, Y., et al. (2022). Rapid acidification of the arctic Chukchi Sea waters driven by anthropogenic forcing and biological carbon recycling. *Geophysical Research Letters*, 49(4), 1–12. https://doi.org/10.1029/2021GL097246
- Ricke, O., Arthun, M., & Dörr, J. S. (2023). Rapid sea ice changes in the future Barents Sea. *The Cryosphere*, 17(4), 1445–1456. https://doi.org/10.
- Shen, Z., Duan, A., Li, D., & Li, J. (2021). Assessment and ranking of climate models in arctic sea ice cover simulation: From CMIP5 to CMIP6. Journal of Climate, 34(9), 3609–3627. https://doi.org/10.1175/JCLI-D-20-0294.1

PENG ET AL.

- Shen, Z., Zhou, W., Li, J., & Chan, J. C. L. (2023). A frequent ice-free arctic is likely to occur before the mid-21st century. *Npj Climate and Atmospheric Science*, 6(1), 103. https://doi.org/10.1038/s41612-023-00431-1
- Shiogama, H., Watanabe, M., Kim, H., & Hirota, N. (2022). Emergent constraints on future precipitation changes. *Nature*, 602(7898), 612–616. https://doi.org/10.1038/s41586-021-04310-8
- Stroeve, J., & Notz, D. (2018). Changing state of arctic sea ice across all seasons. Environmental Research Letters, 13(10), 103001. https://doi.org/10.1088/1748-9326/aade56
- Strople, L. C., Vieweg, I., Yadetie, F., Odei, D. K., Thorsen, A., Karlsen, O. A., et al. (2023). Spawning time in adult polar cod (boreogadus Saida) altered by crude oil exposure, independent of food availability. *Journal of Toxicology and Environmental Health Part A: Current Issues*, 88(2), 43–66. https://doi.org/10.1080/15287394.2023.2228535
- Sun, J., Liu, S., Cohen, J., & Yu, S. (2022). Influence and prediction value of arctic sea ice for spring Eurasian extreme heat events. *Communications Earth & Environment*, 3(1), 172. https://doi.org/10.1038/s43247-022-00503-9
- Terhaar, J., Kwiatkowski, L., & Bopp, L. (2020). Emergent constraint on Arctic Ocean acidification in the twenty-first century. *Nature*, 582(7812), 379–383. https://doi.org/10.1038/s41586-020-2360-3
- Tian, Y., Zhang, Y., Zhong, D., Zhang, M., Li, T., Xie, D., & Wang, G. (2022). Atmospheric energy sources for winter sea ice variability over the north barents–kara seas. *Journal of Climate*, 35(16), 5379–5398. https://doi.org/10.1175/JCLI-D-21-0652.1
- Toxværd, K., Dinh, K. V., Henriksen, O., Hjorth, M., & Nielsen, T. G. (2019). Delayed effects of pyrene exposure during overwintering on the arctic copepod Calanus hyperboreus. *Aquatic Toxicology*, 217, 105332. https://doi.org/10.1016/j.aquatox.2019.105332
- Varpe, Ø., Daase, M., & Kristiansen, T. (2014). A fish-eye view on the new Arctic lightscape. *ICES Journal of Marine Science*, 72(9), 2532–2538. https://doi.org/10.1093/icesims/fsv129
- Vihma, T. (2014). Effects of Arctic Sea ice decline on weather and climate: A review. Surveys in Geophysics, 35(5), 1175–1214. https://doi.org/10.1007/s10712-014-9284-0
- Xu, M., Tian, W., Zhang, J., Wang, T., & Qie, K. (2021). Impact of sea ice reduction in the barents and kara seas on the variation of the East Asian trough in late winter. *Journal of Climate*, 34(3), 1081–1097. https://doi.org/10.1175/JCLI-D-20-0205.1
- Yamagami, Y., Watanabe, M., Mori, M., & Ono, J. (2022). Barents-Kara sea-ice decline attributed to surface warming in the Gulf Stream. *Nature Communications*, 13(1), 3767. https://doi.org/10.1038/s41467-022-31117-6
- Yao, L., Leng, G., Yu, L., Li, H., Tang, Q., Python, A., et al. (2025). Emergent constraints on global soil moisture projections under climate
- change. Communications Earth & Environment, 6(1), 1–8. https://doi.org/10.1038/s43247-025-02024-7
 Zhang, P., Chen, G., Ting, M., Ruby Leung, L., Guan, B., & Li, L. (2023). More frequent atmospheric rivers slow the seasonal recovery of Arctic
- sea ice. Nature Climate Change, 13(3), 266–273. https://doi.org/10.1038/s41558-023-01599-3
 Zhang, P., Wu, Y., Simpson, I. R., Smith, K. L., Zhang, X., De, B., & Callaghan, P. (2018a). A stratospheric pathway linking a colder Siberia to
- Barents-Kara Sea sea ice loss. *Science Advances*, 4(7), 1–8. https://doi.org/10.1126/sciadv.aat6025
- Zhang, P., Wu, Y., & Smith, K. L. (2018b). Prolonged effect of the stratospheric pathway in linking barents-kara sea sea ice variability to the midlatitude circulation in a simplified model. Climate Dynamics, 50(1-2), 527-539. https://doi.org/10.1007/s00382-017-3624-y
- Zhu, H., Jiang, Z., Li, L., Li, W., & Jiang, S. (2024). Improve the projection of east China summer precipitation with emergent constraints. *Npj Climate and Atmospheric Science*, 7(1), 1–9. https://doi.org/10.1038/s41612-024-00863-3

PENG ET AL.